Indoor Particulate Matter of Outdoor Origin: Importance of Size-Dependent Removal Mechanisms

Article *in* Environmental Science and Technology · February 2002

DOI: 10.1021/es010723y · Source: PubMed

4 authors, including:

William Riley
Lawrence Berkeley National Laboratory
385 PUBLICATIONS **12,614** CITATIONS

SEE PROFILE

Environ. Sci. Technol. **2002**, *36,* 200−207

Indoor Particulate Matter of Outdoor Origin: Importance of Size-Dependent Removal Mechanisms

WILLIAM J. RILEY,*,† THOMAS E. MCKONE,†,‡ ALVIN C. K. LAI,†,§ AND WILLIAM W. NAZAROFF||

Indoor Environment Department, Environmental Energy Technologies Division, E.O. Lawrence Berkeley National Laboratory, 1 Cyclotron Road, Berkeley, California 94720, and School of Public Health and Department of Civil and Environmental Engineering, University of California, Berkeley, California, 94720

Adverse human health effects have been observed to correlate with levels of outdoor particulate matter (PM), even though most human exposure to PM of outdoor origin occurs indoors. In this study, we apply a model and empirical data to explore the indoor PM levels of outdoor origin for two major building types: offices and residences. Typical ventilation rates for each building type are obtained from the literature. Published data are combined with theoretical analyses to develop representative particle penetration coefficients, deposition loss rates, and ventilation-system filter efficiencies for a broad particle size range (i.e., 0.001−10 μm). We apply archetypal outdoor number, surface area, and mass PM size distributions for both urban and rural airsheds. We also use data on mass-weighted size distributions for specific chemical constituents of PM: sulfate and elemental carbon. Predictions of the size-resolved indoor proportion of outdoor particles (IPOP) for various conditions and ambient particle distributions are then computed. The IPOP depends strongly on the ambient particle size distribution, building type and operational parameters, and PM metric. We conclude that an accurate determination of exposure to particles of ambient origin requires explicit consideration of how removal processes in buildings vary with particle size.

Introduction

Recent epidemiological studies have shown strong correlations between elevated outdoor particulate matter (PM) levels and a range of adverse health effects, including early mortality (*1, 2*), exacerbation of respiratory tract disease, reduced lung function (*3*), and cardiovascular disease (*4, 5*). The mechanisms by which PM exposure affects human health are unclear and are the subject of much current research (*6*).

Understanding the impact of outdoor PM on human health requires recognition that people spend a large fraction (∼90%) of their time indoors (*7, 8*). Indeed, recent studies indicate that most of the population exposure to PM occurs in buildings (*9, 10*). These studies show that indoor particle concentrations can be attributed to both outdoor and indoor sources. Particle removal by a ventilation-system filter, deposition to the building shell during air infiltration, and deposition onto indoor surfaces can significantly affect the indoor concentration of particles originating outdoors (*11*). These loss processes vary with building conditions and operation and are strongly particle-size dependent. An understanding of how the outdoor PM properties are modified indoors is needed to accurately estimate human exposure based on ambient measurements.

Until recently, studies designed to understand relationships between indoor and outdoor PM levels focused on integral measures of PM without size discrimination (*12, 13*). Furthermore, the integrated PM measurements have often mixed PM originating outdoors with contributions from indoor sources. More recent studies (*14*−*19*) have attempted to differentiate indoor−outdoor concentration ratios based on particle size and to separate indoor and outdoor sources. In this paper, we expand on such studies by specifically treating building operational characteristics (i.e., filtration, penetration, deposition, and ventilation) and their size-dependent effects on indoor PM levels. We apply this approach to determine the size-resolved indoor particle concentrations of outdoor origin for several potential health metrics, including number and surface area concentrations, $PM_{2.5}$ and PM_{10} mass concentrations, and selected chemical species. We also perform analyses for characteristic rural and urban PM size distributions.

Methods

Indoor Proportion of Outdoor Particles. Figure 1 illustrates the modeled processes that affect the indoor proportion of outdoor particles (IPOP). The model complexity was chosen to match the data available for parametrization and is based on work by Alzona et al. (*20*). This approach to modeling indoor PM levels has also been applied in studies by Nazaroff and Cass (*21*) and Leaderer et al. (*22*), among others. Assuming isothermal conditions, no resuspension or coagulation of particles, and no phase change processes, the size-specific mass balance for particles of outdoor origin is

$$\frac{\mathrm{d}(CV)}{\mathrm{d}t} = Q_{\mathrm{m}}C_{\mathrm{o}}(1-\eta_{\mathrm{m}}) + Q_{\mathrm{n}}C_{\mathrm{o}} + pQ_{\mathrm{i}}C_{\mathrm{o}} - Q_{\mathrm{r}}\eta_{\mathrm{r}}C - C\sum_j v_{\mathrm{d},j}S_j - (Q_{\mathrm{m}} + Q_{\mathrm{i}} + Q_{\mathrm{n}})C \quad (1)$$

where C_{o} is the outdoor PM concentration (μg m^{-3}); C is the indoor concentration of PM of outdoor origin (μg m^{-3}); t is time (s); j is an index referencing each of the three major surface orientations in the building (upward facing, downward facing, and vertical); $v_{\mathrm{d},j}$ is the deposition velocity for orientation j (m s^{-1}); S_j is the surface area with orientation j (m^2); η_{m} and η_{r} are the makeup and recirculation filter efficiencies, respectively; p is the particle penetration factor; V is the room volume (m^3); and Q_{m}, Q_{r}, Q_{n}, and Q_{i} are the makeup, recirculation, natural ventilation, and infiltration airflow rates (m^3 s^{-1}), respectively. Natural ventilation refers

* Corresponding author phone: (510)486-5036; fax: (510)486-7070; e-mail: wjriley@lbl.gov.

† E. O. Lawrence Berkeley National Laboratory.

‡ School of Public Health, University of California, Berkeley.

§ Present address: School of Mechanical and Production Engineering, Nanyang Technological University, 50 Nanyang Ave., Singapore 639798.

|| Department of Civil and Environmental Engineering, University of California, Berkeley.

10.1021/es010723y CCC: $22.00
Published on Web 12/13/2001

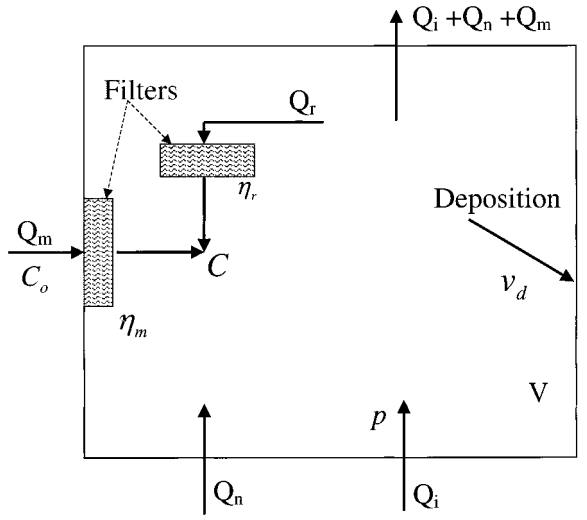

FIGURE 1. Schematic of the processes that affect the indoor proportion of outdoor particles for a generic single-zone building. See text for symbol definitions.

to airflow through open windows and doors, while infiltration refers to airflow through the remainder of the building shell. Applying a time average to eq 1 while neglecting the change of PM mass within the building and assuming that C_o and C are not correlated in time with Q_m, Q_r, Q_i, Q_n, or $v_{d,j}$ yields

$$\frac{C}{C_o} = \frac{\frac{Q_m}{V}(1-\eta_m) + \frac{Q_n}{V} + \frac{pQ_i}{V}}{\frac{Q_r\eta_r}{V} + \beta + \frac{Q_m + Q_i + Q_n}{V}} \quad (2)$$

where C/C_o is the size-specific, time-averaged IPOP and β is the deposition loss rate coefficient (s^{-1}), defined as $\sum(v_{d,j}S_j)/V$. For simplicity, in the calculations that follow we assume that the makeup and recirculation filter efficiencies are equivalent (i.e., $\eta_m = \eta_r$). Equation 2 also describes the size-specific IPOP for a particular chemical constituent of PM. Although the form of eq 2 is the same as that obtained by assuming that steady-state conditions apply, the terms in eq 2 represent time averages and not instantaneous values. Assuming uncorrelated ventilation rates and particle concentrations is an important restriction on eq 2. However, this restriction is less severe than those imposed by a steady-state assumption, which requires that all input parameters be constant in time. Because we are most interested in illustrating the importance of the PM size distribution, we believe that the model assumptions do not unduly limit the value of the work presented here.

The analysis in this paper does not consider indoor sources. It is well-known that indoor sources exist and can contribute significantly to indoor PM levels. In particular, environmental tobacco smoke, cooking, and cleaning activities are important indoor particle sources (*23*). We focus on the indoor proportion of outdoor particles and exclude indoor sources since the epidemiological literature has focused on health effects associated with ambient particle levels. The methods and concepts developed here can be extended to the study of indoor PM sources, but such an effort will require a more thorough characterization of these sources.

Resuspension would increase the time-averaged IPOP above that calculated by eq 2; this effect would be most pronounced for coarse mode particles (*24*). Models have been developed to estimate resuspension rates (*25*), but more research is required to thoroughly characterize this effect. We do not include the effects of resuspension in the current study.

Building Simulation Scenario. We considered five representative building scenarios: (i) an office building with a 40% ASHRAE filter (Ofc40); (ii) an office building with an 85% ASHRAE filter (Ofc85); (iii) a closed residence with continuous central air and a standard furnace filter (ResCA); (iv) a residence with a typical infiltration ventilation rate and no central air (ResTV); and (v) a residence with a high natural ventilation rate as may occur with open windows (ResHV). For the office building scenarios, we applied the results of Persily (*26*), who reported makeup ventilation rates for 14 U.S. office buildings (Table 1). Murray and Burmaster (*27*) reported on a set of 2844 measurements of U.S. residential ventilation rates. For the ResTV scenario, we used their geometric mean (GM) and standard deviation (GSD) of the full data set; for the ResHV scenario, we applied the 95th percentile ventilation rate. The remaining ventilation parameters in Table 1 were chosen based on the authors' scientific judgment. In cases where we did not have information on ventilation rate variability, we assumed the distribution to be lognormal with a default GSD of 1.5.

Filtration Efficiency. Hanley et al. (*28*) measured the removal efficiency of several filters for particles with diameters between 0.01 and 2.4 μm. In the current study, we use their data for loaded home furnace filters and two commonly used commercial filters: the 40% and 85% ASHRAE filters (*29*). We applied fibrous-bed filtration theory to augment these results for particles smaller than 0.01 μm and larger than 2.4 μm (*30*). We generated a best fit to the Hanley et al. (*28*) data set by minimizing the log-squared difference between theoretical and measured removal efficiencies. Bed solidity and fiber diameter were used as fitting parameters. We were unable to fit the filter efficiency data over the entire range of particle diameters with a single combination of solidity and fiber diameter. Therefore, different fits were generated to apply for particles with diameters less than 0.01 μm and greater than 2.4 μm for each filter (Figure 2). Linear interpolation between measured data was used for particles with diameters between 0.01 and 2.4 μm.

Deposition. Our deposition model is based on results from experimental studies (*31*−*36*) that measured the indoor deposition loss rate over a range of particle sizes, ventilation conditions, and indoor surface area to volume ratios. We characterize a representative indoor deposition loss rate coefficient across a broad particle size range by extending these experimental results using a theoretical analysis for ultrafine particles. Experimental results are summarized in Figure 3, along with a least-squares cubic polynomial fit to the logarithmically transformed data. We applied the smooth indoor surface particle deposition theory of Lai and Nazaroff (*37*) to estimate deposition for particles with diameters smaller than 0.06 μm. For this analysis, we used a surface area to volume ratio of 3 m^{-1}, which is a typical value in furnished rooms (*38*). The theoretical loss rate coefficient for ultrafine particles onto smooth surfaces is a function of the shear velocity. To match the curve fit to the empirical data at a particle diameter of 0.06 μm required a shear velocity of 3.0 cm s^{-1}, a value within the range of expected shear velocities in indoor spaces.

PM Penetration. We define the particle penetration factor (p) as the fraction of particles of a specific diameter that pass through the building shell along with infiltrating air. Substantial uncertainty in the penetration factor exists in the literature. Two studies indicate that p is close to 1.0 for a wide range of particle diameters (*13, 24*), while several recent studies (*14, 18, 19, 39*) have presented data indicating that the penetration factor may be significantly less than 1 and varies with particle size.

In the current study, we use a baseline value for p defined by the idealized crack theory of Liu and Nazaroff (*40*). The

TABLE 1. Geometric Mean (GSD) Ventilation Parameters for Each Building Scenario[a]

	building type and operation			
parameter	Ofc40 and Ofc85	ResCA	ResTV	ResHV
Q_m/V (h^{-1})	0.73 (1.8)[b]	0	0	0
Q_r/V (h^{-1})	3 (1.5)	4 (1.5)	0	0
Q_n/V (h^{-1})	0	0	0	2.2[d] (1.5)
Q_i/V (h^{-1})	0.25 (1.5)	0.75 (1.5)	0.53 (2.27)[c]	0
filter	40 or 85% ASHRAE (1.5[e])	standard furnace filter (1.5[e])	na [f]	na

[a] Q_m, Q_r, Q_n, and Q_i are the makeup, recirculation, natural ventilation, and infiltration airflow rates, respectively. Ofc40 and Ofc85, office buildings. ResCA, residence closed with continuous central air. ResTV, residence closed with typical ventilation. ResHV, residence with high air exchange rate. [b] Estimated from Figure 19 of ref *26*. [c] GM and GSD for full data set (*27*). [d] 95% percentile value (*27*). [e] Filter efficiencies are limited to be lower than 1.0 in the Monte Carlo simulations. [f] na, not applicable.

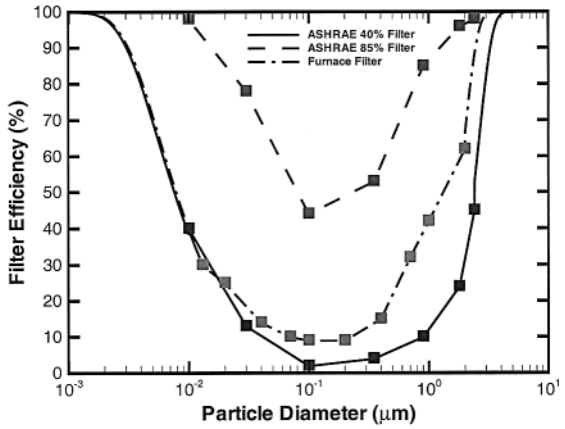

FIGURE 2. Filter efficiency vs particle size, as predicted from the data of Hanley et al. (*28*) (squares) and extrapolated using the theory of Hinds (*30*).

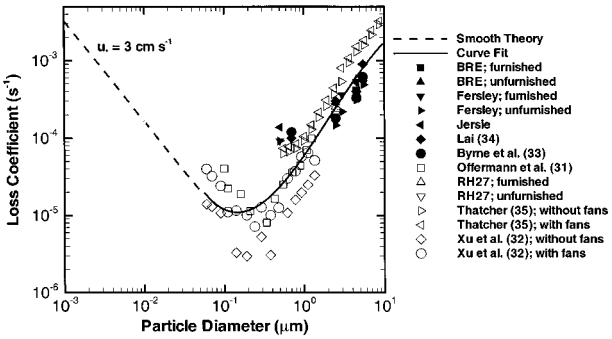

FIGURE 3. Deposition loss rate coefficient (β) vs particle size. Shown are the data sets referenced in the text, a least-squares third-order polynomial fit to the log-transformed data, and predictions for particle diameters less than 0.06 μm from the smooth indoor surface particle deposition theory of Lai and Nazaroff (*37*).

theory assumes idealized rectangular cracks with regular geometry, smooth inner surfaces, and steady airflow. Deposition occurs by gravitational settling, Brownian diffusion, and inertial impaction. In the model, we assume a mean crack height of 0.8 mm, a crack flow length of 9 cm, a total crack length throughout the building shell of 1000 m, and a 4 Pa pressure drop across the building shell. This combination of parameters results in a penetration factor that closely matches the experimental results presented in Long et al. (*14*) for one house (their Figure 7b). In real buildings, crack size, length, and geometry can vary substantially. The large uncertainty in the particle penetration factor implies a need to better characterize this parameter. Our model structure easily permits analysis of the effect of p on the predicted IPOP as more information on this parameter becomes available.

Outdoor PM Concentrations. Jaenicke (*41*) described archetypal atmospheric aerosol size distributions as the sums of three lognormal distributions. By combining PM distributions from a number of studies, he developed parameters to describe several distributions; in this study, we apply his approximations for PM distributions in rural and urban areas (Table 2). With a particle density, ρ (g cm^{-3}), of 1 g cm^{-3}, the integrated $PM_{2.5}$ and PM_{10} mass concentrations for the urban distribution are 43 and 60 μg m^{-3}, respectively, and for the rural distribution are 12 and 59 μg m^{-3}, respectively.

Because of differences in sources, particle density may not be constant across the particle size distribution. Coarse particles consist of soil dust and other mechanically generated material, while fine mode particles contain primary particles from combustion sources and secondary aerosol material (*42*). Thus, smaller particles will have densities closer to 1 g cm^{-3}, while larger particles may have densities closer to that of soil grains (i.e., 2.5 g cm^{-3}). However, there is insufficient information in the literature to accurately characterize ambient particle density as a function of size. For the results presented here, we take the particle density to be 1 g cm^{-3}. To estimate the impact of particle density variability on the IPOP, we make comparisons to a binary density distribution with fine mode particles having a density of 1 g cm^{-3} and coarse mode particles having a density of 2.5 g cm^{-3}.

Because human health effects of ambient PM may depend on particle composition as well as size distribution, we developed IPOP relationships for particles of different composition. We present results here for two constituents: sulfate and elemental carbon.

Whitby (*43*) compiled data from 5 studies of 15 urban sites to characterize the size composition of sulfate in atmospheric aerosol. He summarizes the size composition data as a single log-normal distribution, with a geometric mean particle diameter ($D_{pm} = 0.48 \pm 0.10\,\mu$m) and geometric standard deviation ($\sigma_g = 2.0 \pm 0.29$).

Offenberg and Baker (*44*) measured elemental carbon (EC) and organic carbon (OC) during the summer and winter in Chicago. Several studies have linked EC levels with human health effects (e.g., ref *45*). In the current work, we include an estimate of the IPOP for the winter EC size distribution as ambient EC levels tend to be highest in the winter. The measured particle size distributions we applied are summarized as follows: for $D_p = 0.15$, 0.45, 1.4, 4.1, and 12.2 μm, respectively, the values of the normalized elemental carbon mass size distribution ($\Delta C/[C_{total}\Delta \log D_p]$) were 0.0, 0.49, 0.73, 0.49, and 0.19.

Integral PM Measures. We compute integrated number (N, m^{-3}), surface area (A, μm^2 m^{-3}), and mass (M, μg m^{-3}) concentrations for three particle size ranges [$D_p \le 10\,\mu$m (PM_{10}), $D_p \le 2.5\,\mu$m ($PM_{2.5}$), and $2.5\,\mu m \le D_p \le 10\,\mu$m (coarse mode)] by numerically integrating the appropriately weighted moment of the size distribution over the respective particle size range. We also compute the effective integrated $PM_{2.5}$ and PM_{10} recirculation and makeup filter efficiencies and

TABLE 2. Mean Diameters and Standard Deviations of the Three Lognormal Modes for Characteristic Aerosol Distributions in Rural and Urban Areas (*41*)

	mode I			mode II			mode III			integral measures	
type	N_i (cm^{-3})	D_{pi} (μm)	log σ_i (−)	N_i (cm^{-3})	D_{pi} (μm)	log σ_i (−)	N_i (cm^{-3})	D_{pi} (μm)	log σ_i (−)	$PM_{2.5}$ mass[a] ($\mu g\ m^{-3}$)	PM_{10} mass[a] ($\mu g\ m^{-3}$)
urban	9.93×10^4	0.013	0.245	1.1×10^3	0.014	0.666	3.64×10^4	0.05	0.337	43	60
rural	6650	0.015	0.225	147	0.054	0.557	1990	0.084	0.266	12	59

[a] Assuming a particle density of 1 g cm^{-3}.

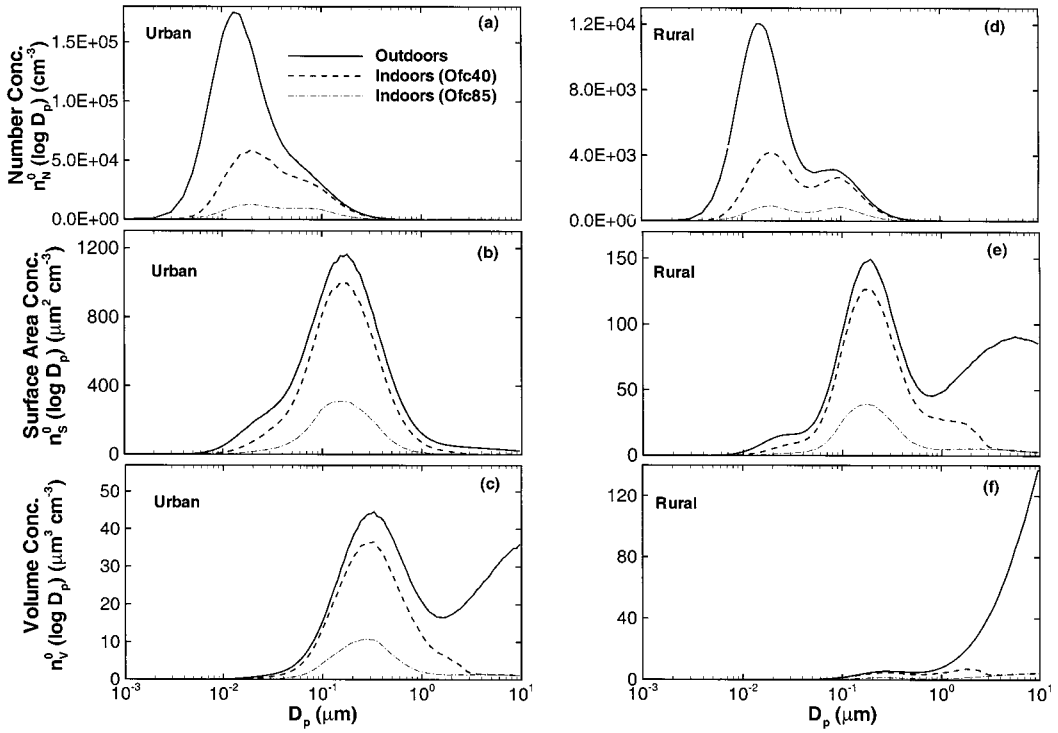

FIGURE 4. Archetypal urban and rural aerosol distributions and predicted indoor particle number, surface area, and volume concentrations for the office building with 40% (Ofc40) and 85% (Ofc85) ASHRAE filters. Panels a−c show number, surface area, and volume distributions, respectively, for urban aerosol; panels d−f show the corresponding distributions for rural aerosol.

particle deposition velocity for each scenario by integrating the mass-weighted filtration efficiency over the appropriate particle size ranges.

The integrated parameters differ among simulation scenarios because of changes in the outdoor PM size distribution. These integrated measures can be useful for estimating the IPOP for integral measures of PM in the absence of a size-dependent characterization of ambient PM, penetration, deposition loss rate, or filter performance.

Addressing Uncertainty. Because of limitations in the data and theories to support IPOP modeling, there is a need to characterize uncertainty and variability in the model approach and input parameters. The framework for the analysis of uncertainty in human exposure and health risk assessment developed by Morgan and Henrion (*46*) and Cullen and Frey (*47*) distinguishes among parameter uncertainty, model uncertainty, and decision rule uncertainty and calls for a separate treatment of these different types of uncertainty. In the current study, we explicitly address parameter uncertainty.

We apply a Monte Carlo approach to estimate the impact of parameter uncertainty on our IPOP predictions. Lognormal distributions are used to represent building ventilation rates, and when possible, literature values are used to obtain the characteristics of the distribution. In cases where literature data were inconclusive or unavailable, we used scientific judgment to obtain distribution characteristics. To express uncertainty in outdoor particle concentrations, particle penetration, filter efficiency, and deposition loss rate parameters, we used lognormal distributions with a GSD of 1.5 and a GM based on available data. Parameter values sampled from the distributions were limited to a range defined by a factor of 2.5 from the GM, and the filter efficiency and penetration rate were limited to values below 1. For this study, the Monte Carlo results were computed from an ensemble of 1000 model simulations.

Results and Discussion

Size-Resolved Particulate Matter. Figure 4 illustrates the outdoor and predicted indoor number, surface area, and volume concentrations for the archetypal urban and rural distributions and the two office building scenarios. For clarity, we present only the mean of the Monte Carlo simulations. The overall impact of filtration and deposition differ among the number, surface area, and mass PM distributions because each metric has different size dependence. For example, a large fraction of the number concentration distribution occurs below particle diameters of about 0.05 μm, where both deposition and filtration are efficient removal mechanisms (Figure 4a,d). The urban indoor surface area concentration (Figure 4b) for the building equipped with a 40% ASHRAE filter is relatively unaffected by the building since the removal mechanisms are inefficient in the accumulation

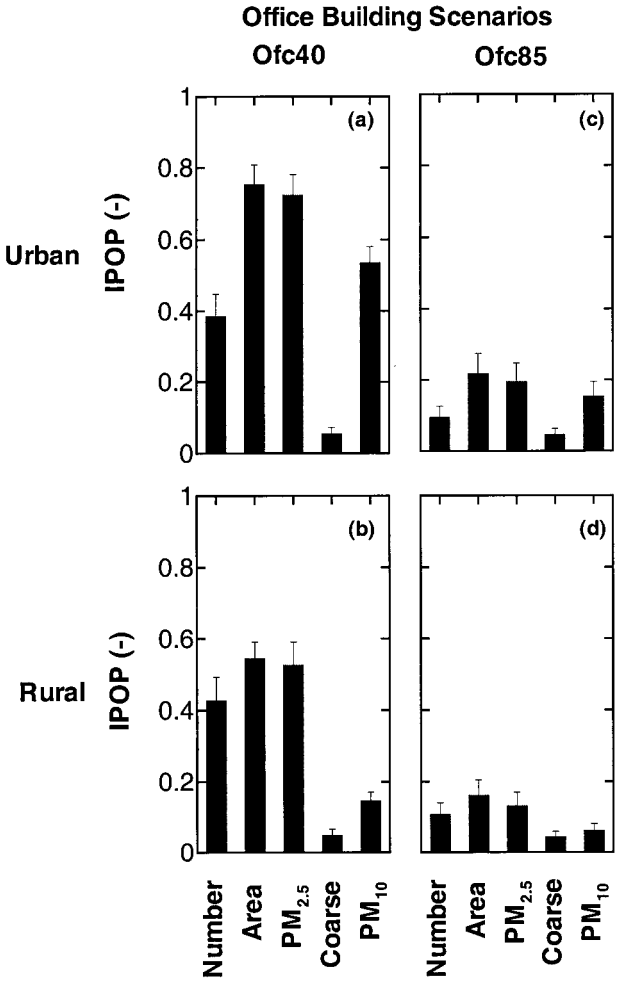

FIGURE 5. Predicted indoor proportion of outdoor particles (IPOP) for the office building with 40% (Ofc40) and 85% (Ofc85) ASHRAE filters and the archetypal urban and rural aerosol distributions. The IPOP values are shown for PM_{10} number, PM_{10} surface area, $PM_{2.5}$ mass, coarse mode mass, and PM_{10} mass.

mode where a large portion of the PM surface area exists. Note that the 85% ASHRAE filter substantially reduces the indoor PM surface area concentration for both rural and urban conditions since this filter is more efficient than the 40% filter in the accumulation mode and because the office building recirculation flow rate is relatively high as compared to the makeup ventilation rate. For the urban distribution, the 85% ASHRAE filter reduces the indoor volume concentration substantially as compared to the 40% filter. Much of the PM volume in the rural scenario is in the coarse mode (Figure 4f), resulting in a large removal of PM_{10} volume in both office building scenarios.

Figure 5 summarizes the office building IPOP predictions. Values range from 0.05 for the coarse mode mass in all four cases to 0.75 for particle surface area with urban PM and a 40% ASHRAE filter. For the archetypal urban atmosphere, the 85% ASHRAE filter reduces all the IPOP values (except the coarse mode mass) by a factor of about 3−4 as compared to the 40% ASHRAE filter (Figure 5a,c). The lesser impact in the coarse mode mass is a result of the high efficiency (>99%) of both filters for particles with diameters greater than about 3 μm (Figure 2).

Figure 6 shows outdoor and predicted mean indoor number, surface area, and volume concentrations for the three residential scenarios. Patterns similar to those in the office building scenarios (Figure 4) are found here. For the ResHV building scenario in both urban and rural atmospheres, the surface area and volume concentrations below ~1 μm are essentially unchanged across the building shell.

Compared to the office building scenarios, the residential scenarios show a larger fraction of the outdoor PM concentration indoors (Figure 7). For the residential scenarios, IPOP values for most metrics are again lower in the rural distribution than in the urban distribution. The largest IPOP values occur for the ResHV scenario where, for the urban PM distribution, PM_{10} number and mass IPOP are above 0.8 while the surface area and $PM_{2.5}$ mass IPOP are above 0.9. The ResCA scenario has the smallest IPOP for both archetypal ambient distributions and for all indoor metrics. Applying the binary particle density (i.e., higher density in the coarse mode) resulted in coarse mode and PM_{10} mass IPOP values between 5 and 20% lower than with the uniform particle density of 1 g cm^{-3}.

Integrated Deposition Loss Coefficient and Filtration Efficiency. Integrated $PM_{2.5}$ and PM_{10} deposition loss rate coefficients and filter efficiencies are presented in Table 3. These parameters differ markedly between $PM_{2.5}$ and PM_{10} integrated values. For example, the Ofc40 scenario in the archetypal urban PM distribution has makeup filter efficiencies of 8% and 31% for the $PM_{2.5}$ and PM_{10} particle size ranges, respectively. Furthermore, for a particular ambient PM distribution and building scenario, the recirculation and makeup filters can have different integrated efficiencies, even though they are identical filters. The recirculation and makeup filters operate on indoor and ambient airstreams, respectively, and these airstreams have different PM size distributions. The largest difference occurs for PM_{10} for the urban particle size distribution and the Ofc40 building scenario where the makeup filter was about four times as efficient as the recirculation filter. Differences between the integrated filter efficiencies were smaller for the Ofc85 scenario since the efficiency of the 85% ASHRAE filter is less variable with particle size than is the 40% filter. The integrated $PM_{2.5}$ recirculation and makeup filter efficiencies are comparable for each scenario.

The integrated PM_{10} deposition loss rate coefficient varies by more than an order of magnitude among the simulated scenarios. Simulations with the urban PM distribution result in smaller PM_{10} deposition loss rate coefficients than with the rural distribution. This observation is consistent with the larger fraction of coarse mode mass in the rural PM size distributions. The integrated deposition loss rate coefficient for $PM_{2.5}$ is smaller than for PM_{10} and varies by a factor of about 3 across scenarios. For comparison, Ozkaynak et al. (*13*) reported mean integrated $PM_{2.5}$ and PM_{10} deposition loss rates of 0.39 and 0.65 h^{-1}, respectively, from the PTEAM study of residences in southern California. Their fitted PM_{10} deposition loss rate is consistent with that found under the urban high ventilation residential scenario presented here. However, their $PM_{2.5}$ integrated deposition loss rate is about three times larger than our predictions. The discrepancy may be due to differences in the outdoor particle size distribution or the inclusion of indoor sources in the PTEAM study data.

These differences suggest that care must be taken when choosing representative values for exposure studies. We emphasize that the recirculation filter efficiency and the deposition loss rate coefficient values for integral PM measures can vary with any parameter that changes the indoor particle size distribution, such as the ventilation rate. Despite these limitations, the information in Table 3 can provide guidance for direct application of a mass balance model of integral PM measures in the absence of size-resolved data.

Simulation Results for Individual Compounds in PM. Table 4 summarizes the IPOP values for $PM_{2.5}$ and PM_{10} fractions of sulfate and elemental carbon. For offices,

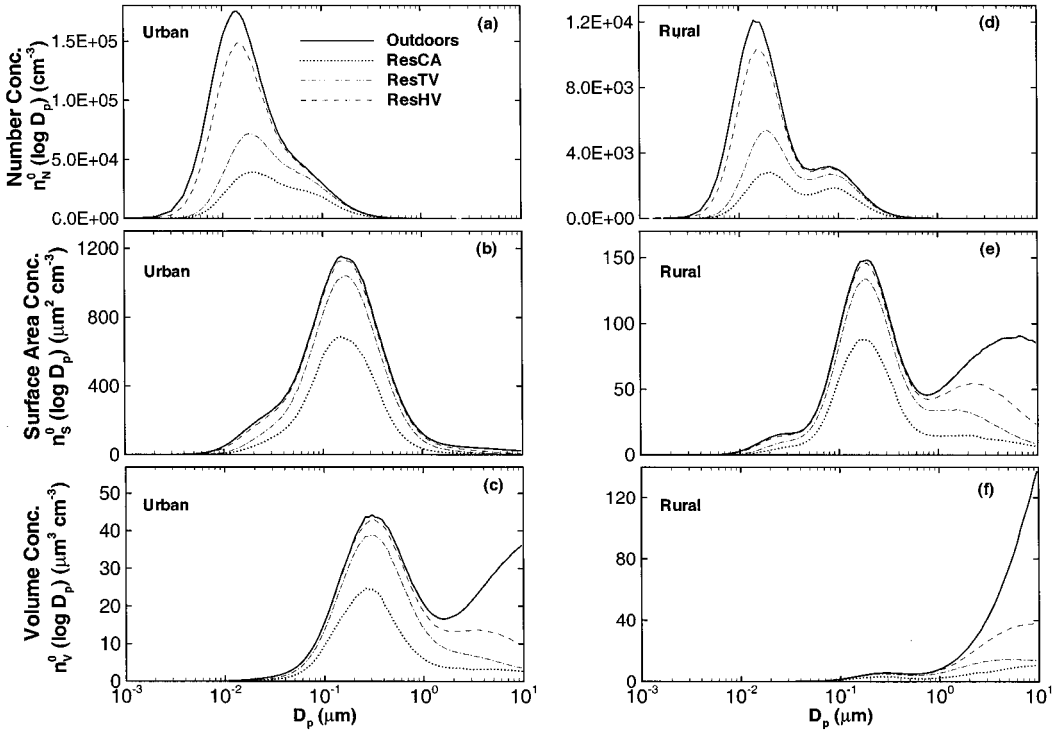

FIGURE 6. Archetypal urban and rural aerosol distributions and predicted indoor particle number, surface area, and volume concentrations for the three residential scenarios (ResCA, closed with central air; ResTV, typical infiltration ventilation; and ResHV, high natural ventilation). Panels a–c show number, surface area, and volume distributions, respectively, for urban aerosol; panels d–f show the corresponding distributions for rural aerosol.

TABLE 3. Mean Integrated $PM_{2.5}$ and PM_{10} Deposition Loss Rate Coefficient and Recirculation and Makeup Filter Efficiencies (SD) for the Archetypal Urban and Rural PM Distributions and the Five Building Scenarios

		$PM_{2.5}$			PM_{10}		
ambient distribution	building scenario	deposition loss rate coeff (h^{-1})	recirculation filter efficiency (%)	makeup filter efficiency (%)	deposition loss rate coeff (h^{-1})	recirculation filter efficiency (%)	makeup filter efficiency (%)
archetypal urban	Ofc40	0.10 (0.01)	6 (0.3)	8 (0.3)	0.17 (0.02)	8 (0.8)	31 (1.0)
	Ofc85	0.09 (0.01)	56 (1.8)	64 (1.5)	0.32 (0.05)	59 (2.0)	72 (1.2)
	ResCA	0.09 (0.01)	19 (0.9)	–[a]	0.32 (0.04)	24 (1.5)	–
	ResTV	0.11 (0.01)	–	–	0.31 (0.10)	–	–
	ResHV	0.13 (0.01)	–	–	0.53 (0.07)	–	–
archetypal rural	Ofc40	0.24 (0.02)	13 (0.9)	19 (1.1)	0.96 (0.2)	32 (4.2)	77 (1.8)
	Ofc85	0.23 (0.03)	67 (2)	79 (1.9)	1.9 (0.2)	81 (2.4)	91 (1.7)
	ResCA	0.25 (0.02)	32 (2)	–	1.9 (0.1)	62 (2.6)	–
	ResTV	0.27 (0.03)	–	–	1.5 (0.3)	–	–
	ResHV	0.33 (0.02)	–	–	2.1 (0.2)	–	–

[a] –, not applicable.

differences in filter efficiency have a large impact on the IPOP for both constituents. For example, with the 40% ASHRAE filter, the sulfate PM_{10} mass IPOP is about 0.72. The more efficient filter (85% ASHRAE) lowers the PM_{10} mass IPOP to 0.18.

In residences, the high ventilation scenario has $PM_{2.5}$ mass IPOP values above 0.9 for both constituents. Filtration and the reduced infiltration rate in the residence with a continuously operating central air handler (ResCA) lowered the PM_{10} and $PM_{2.5}$ mass IPOP values for both species to below 0.5.

Comparison with Empirical Evidence. We identified two recent studies that provide an opportunity for comparison of field observations with our simulation results. Ott et al. (*48*) computed the PM_{10} IPOP for three large-scale field studies of residences by removing the impact of indoor sources on measured indoor PM levels with their random component superposition statistical model. They inferred mean PM_{10} IPOP values for these three studies as 0.54, 0.55, and 0.61, respectively. They did not report IPOP values for $PM_{2.5}$. Because our model is parameterized with deposition loss rates, ventilation rates, and filtration efficiencies based on many studies with varying conditions and we are applying archetypal ambient PM size distributions, we do not expect our IPOP predictions to correspond directly to the results of Ott et al. Nevertheless, our results for the PM_{10} mass IPOP of about 0.4, 0.6, and 0.8 for the urban size distribution and three residential scenarios bracket the values they report. Furthermore, the typical ventilation residential scenario (ResTV) closely matches the results from the field studies.

Ozkaynak et al. (*13*) described results from the PTEAM study of 178 participants in southern California. In addition to PM_{10} measurements, elemental analyses of sulfur were also performed. The mass median diameter of sulfur particles was less than 1 μm; these particles represent a good proxy for $PM_{2.5}$ sulfate. Their data suggest an IPOP of 0.7, which matches the typical ventilation residential scenario (ResTV) predicted IPOP of 0.8 $\pm$ 0.1 well.

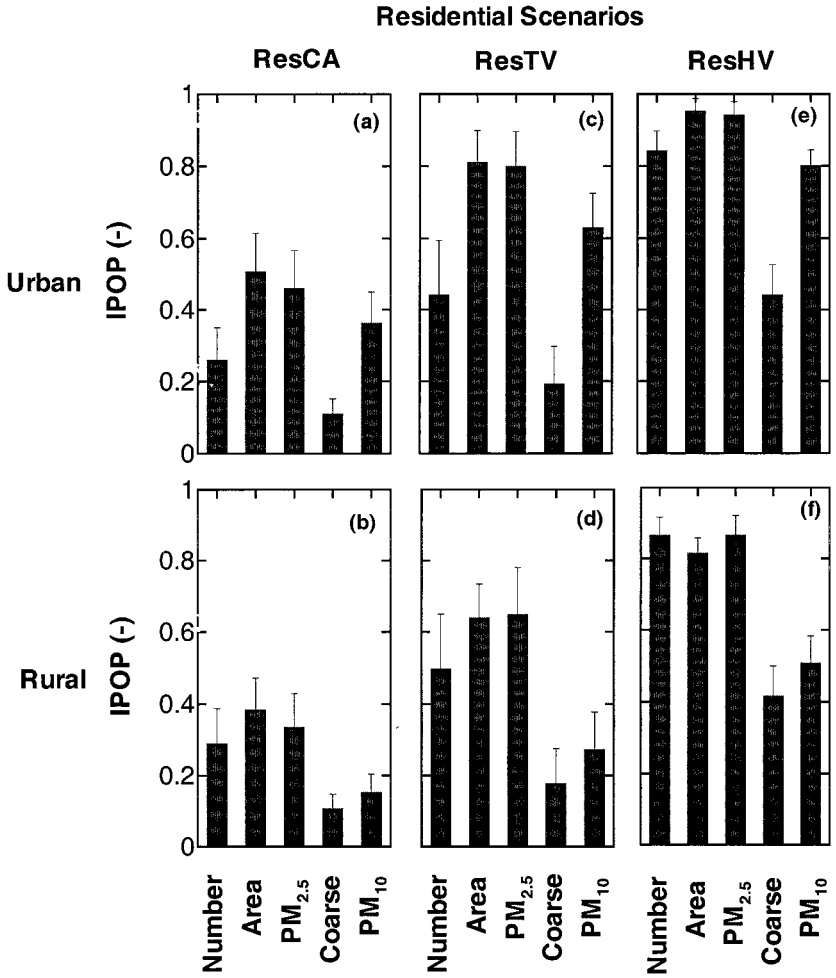

FIGURE 7. Predicted indoor proportion of outdoor particles (IPOP) for the three residential scenarios (ResCA, closed with central air; ResTV, typical infiltration ventilation; and ResHV, high natural ventilation) in the archetypal urban and rural aerosol distributions. The IPOP values are shown for PM_{10} number, PM_{10} surface area, $PM_{2.5}$ mass, coarse mode mass, and PM_{10} mass.

TABLE 4. Predicted Mean Indoor Proportion of Outdoor Particles (IPOP) (SD) for Average Sulfate (*43*) and Elemental C (*44*) for the Five Building Scenarios

		building scenario				
constituent	metric	Ofc40	Ofc85	ResCA	ResTV	ResHV
sulfate	$PM_{2.5}$	0.72 (0.06)	0.18 (0.05)	0.44 (0.11)	0.80 (0.10)	0.95 (0.04)
	PM_{10}	0.72 (0.06)	0.18 (0.05)	0.44 (0.11)	0.80 (0.10)	0.94 (0.04)
elemental carbon	$PM_{2.5}$	0.63 (0.11)	0.15 (0.05)	0.38 (0.11)	0.73 (0.15)	0.91 (0.13)
	PM_{10}	0.53 (0.09)	0.13 (0.04)	0.33 (0.10)	0.64 (0.14)	0.83 (0.11)

In summary, a full understanding of the adverse health effects of airborne particles requires knowledge of how health-related ambient PM metrics are transformed within buildings. Using a variant of a well-established model, in combination with empirical information and theoretical analyses on key parameters, we have shown that IPOP values can vary from 0.05 to more than 0.9. Ambient size distributions of the PM metric and building design and operation play key roles influencing IPOP values and thus have a significant effect on estimates of human exposure. The approach presented here, especially if combined with more complete parameter data, could serve to strengthen epidemiological studies by improving exposure assessment. The methods and information may also contribute to the development and evaluation of risk reduction strategies that are based on modifying exposure by changing building design and operation.

Acknowledgments

This work was supported by the U.S. Environmental Protection Agency (EPA) National Exposure Research Laboratory through Interagency Agreement DW-988-38190-01-0 and carried out at the Lawrence Berkeley National Laboratory (LBNL) through the U.S. Department of Energy under Contract Grant DE-AC03-76SF00098. The authors thank Bill Fisk, David Faulkner, Rich Sextro, and two anonymous reviewers for their constructive comments.

Literature Cited

(1) Schwartz, J.; Dockery, D. W.; Neas, L. M. *J. Air Waste Manage. Assoc.* **1996**, *46*, 927−939.
(2) Klemm, R. J.; Mason, R. M.; Heilig, C. M.; Neas, L. M.; Dockery, D. W. *J. Air Waste Manage. Assoc.* **2000**, *50*, 1215−1222.
(3) Hoek, G.; Dockery, D. W.; Pope, A.; Neas, L.; Roemer, W.; Brunekreef, B. *Eur. Respir. J.* **1998**, *11*, 1307−1311.

(4) Peters, A.; Liu, E.; Verrier, R. L.; Schwartz, J.; Gold, D. R.; Mittleman, M.; Baliff, J.; Oh, J. A.; Allen, G.; Monahan, K.; Dockery, D. W. *Epidemiology* **2000**, *11*, 11−17.
(5) Pope, C. A.; Verrier, R. L.; Lovett, E. G.; Larson, A. C.; Raizenne, M. E.; Kanner, R. E.; Schwartz, J.; Villegas, M.; Gold, D. R.; Dockery, D. W. *Am. Heart J.* **1999**, *138*, 890−899.
(6) Phalen, R. F.; Wolff, R. K. *Aerosol Sci. Technol.* **2000**, *32*, 1−3.
(7) Klepeis, N. E.; Nelson, W. C.; Ott, W. R.; Robinson, J. P.; Tsang, A. M.; Switzer, P.; Behar, J. V.; Hern, S. C.; Engelmann, W. H. *J. Exposure Anal. Environ. Epidemiol.* **2001**, *11*, 231−252.
(8) Jenkins, P. L.; Phillips, T. J.; Mulberg, E. J.; Hui, S. P. *Atmos. Environ.* **1992**, *26*, 2141−2148.
(9) Lioy, P. J.; Waldman, J. M.; Greenberg, A.; Harkov, R.; Pietarinen, C. *Arch. Environ. Health* **1988**, *43*, 304−312.
(10) Wallace, L. *Risk Anal.* **1993**, *13*, 135−139.
(11) Wallace, L. *Aerosol Sci. Technol.* **2000**, *32*, 15−25.
(12) Yocum, J. E. *JAPCA* **1982**, *32*, 500−520.
(13) Ozkaynak, H.; Xue, J.; Spengler, J.; Wallace, L.; Pellizzari, E.; Jenkins, P. *J. Exposure Anal. Environ. Epidemiol.* **1996**, *6*, 57−78.
(14) Long, C. M.; Suh, H. H.; Catalano, P. J.; Koutrakis, P. *Environ. Sci. Technol.* **2001**, *35*, 2089−2099.
(15) Koponen, I. K.; Asmi, A.; Keronen, P.; Puhto, K.; Kulmala, M. *Atmos. Environ.* **2001**, *35*, 1465−1477.
(16) Abt, E.; Suh, H. H.; Catalano, P.; Koutrakis, P. *Environ. Sci. Technol.* **2000**, *34*, 3579−3587.
(17) Jones, N. C.; Thornton, C. A.; Mark, D.; Harrison, R. M. *Atmos. Environ.* **2000**, *34*, 2603−2612.
(18) Vette, A. F.; Rea, A. W.; Lawless, P. A.; Rodes, C. E.; Evans, G.; Highsmith, V. R.; Sheldon, L. *Aerosol Sci. Technol.* **2001**, *34*, 118−126.
(19) Thornburg, J.; Ensor, D. S.; Rodes, C. E.; Lawless, P. A.; Sparks, L. E.; Mosley, R. B. *Aerosol Sci. Technol.* **2001**, *34*, 284−296.
(20) Alzona, J.; Cohen, B. L.; Rudolph, H.; Jow, H. N.; Frohliger, J. O. *Atmos. Environ.* **1979**, *13*, 55−60.
(21) Nazaroff, W. W.; Cass, G. R. *Atmos. Environ.* **1991**, *25A*, 841−852.
(22) Leaderer, B. P.; Cain, W. S.; Isseroff, R.; Berglund, L. G. *Atmos. Environ.* **1984**, *18*, 99−106.
(23) Yakovleva, E.; Hopke, P. K.; Wallace, L. *Environ. Sci. Technol.* **1999**, *33*, 3643−3650.
(24) Thatcher, T. L.; Layton, D. W. *Atmos. Environ.* **1995**, *29*, 1487−1497.
(25) Schneider, T.; Kildeso, J.; Breum, N. O. *Build. Environ.* **1999**, *34*, 583−595.
(26) Persily, A. Presented at the IAQ '89 Conference, Atlanta, GA, 1989.
(27) Murray, D. M.; Burmaster, D. E. *Risk Anal.* **1995**, *15*, 459−465.
(28) Hanley, J. T.; Ensor, D. S.; Smith, D. D.; Sparks, L. E. *Indoor Air* **1994**, *4*, 169−178.
(29) ASHRAE. *ASHRAE Handbook: Fundamentals*; American Society of Heating, Refrigerating, and Air-Conditioning Engineers: Atlanta, GA, 1993.
(30) Hinds, W. C. *Aerosol Technology: Properties, Behavior, and Measurement of Airborne Particles*, 2nd ed.; Wiley: New York, 1999.
(31) Offermann, F. J.; Sextro, R. G.; Fisk, W. J.; Grimsrud, D. T.; Nazaroff, W. W.; Nero, A. V.; Revzan, K. L.; Yater, J. *Atmos. Environ.* **1985**, *19*, 1761−1771.
(32) Xu, M. D.; Nematollahi, M.; Sextro, R. G.; Gadgil, A. J.; Nazaroff, W. W. *Aerosol Sci. Technol.* **1994**, *20*, 194−206.
(33) Byrne, M. A.; Goddard, A. J. H.; Lange, C.; Roed, J. *J. Aerosol Sci.* **1995**, *26*, 645−653.
(34) Lai, A. C. K. Ph.D. Dissertation, Imperial College of Science, Technology and Medicine, University of London, 1997.
(35) Thatcher, T. L.; Lai, A. C. K.; Moreno-Jackson, R.; Sextro, R. G.; Nazaroff, W. W. *Atmos. Environ.* (submitted for publication).
(36) Fogh, C. L.; Byrne, M. A.; Roed, J.; Goddard, A. J. H. *Atmos. Environ.* **1997**, *31*, 2193−2203.
(37) Lai, A. C. K.; Nazaroff, W. W. *J. Aerosol Sci.* **2000**, *31*, 463−476.
(38) Knutson, E. O. In *Radon and Its Decay Products in Indoor Air*; Nazaroff, W. W., Nero, A. V., Eds.; John Wiley and Sons: New York, 1988; pp 161−202.
(39) Mosley, R. B.; Greenwell, D. J.; Sparks, L. E.; Guo, Z.; Tucker, W. G.; Fortmann, R.; Whitfield, C. *Aerosol Sci. Technol.* **2001**, *34*, 127−136.
(40) Liu, D.; Nazaroff, W. W. *Atmos. Environ.* **2001**, *35*, 4451−4462.
(41) Jaenicke, R. In *Aerosol−Cloud−Climate Interactions*; Hobbs, P. V., Ed.; Academic Press: San Diego, CA, 1993; pp 1−31.
(42) Seinfeld, J. H.; Pandis, S. N. *Atmospheric Chemistry and Physics: From Air Pollution to Climate Change*; Wiley: New York, 1998.
(43) Whitby, K. T. *Atmos. Environ.* **1978**, *12*, 135−159.
(44) Offenberg, J. H.; Baker, J. E. *Atmos. Environ.* **2000**, *34*, 1509−1517.
(45) Finlayson-Pitts, B. J.; Pitts, J. N. *Chemistry of the Upper and Lower Atmosphere: Theory, Experiments, and Applications*; Academic Press: San Diego, CA, 2000.
(46) Morgan, M. G.; Henrion, M. *Uncertainty: A Guide to Dealing with Uncertainty in Quantitative Risk and Policy Analysis*; Cambridge University Press: Cambridge, U.K., 1990.
(47) Cullen, A. C.; Frey, H. C. *Probabilistic Techniques in Exposure Assessment*; Plenum Press: New York, 1999.
(48) Ott, W.; Wallace, L.; Mage, D. *J. Air Waste Manage. Assoc.* **2000**, *50*, 1390−1406.

Received for review March 9, 2001. Revised manuscript received September 17, 2001. Accepted October 22, 2001.

ES010723Y